OG H.2-9

ABUNDANCES OF COSMIC RAY NUCLEI HEAVIER THAN $_{50}$Sn

C.J. Waddington and R.K. Fickle, School of Physics and Astronomy, University of Minnesota, Mpls., MN 55455, U.S.A.;
T.L. Garrard and E.C. Stone, 220-47 Downs Laboratory, California Institute of Technology, Pasadena, CA 91125, U.S.A.;
W.R. Binns, M.H. Israel and J. Klarmann, Department of Physics, Washington University, St. Louis, MO 63130, U.S.A.

ABSTRACT

Preliminary results are reported from 430 days of exposure of the heavy nuclei experiment on the HEAO-3 spacecraft. These results are confined to the heavy nuclei with $Z \geq 50$ and emphasize the conclusions obtained on the relative numbers of actinides and heavy stable elements in the lead-platinum region. The extreme paucity of actinides found is inconsistent with the predictions of a cosmic ray source that is highly enriched in r-process material, but quite consistent with a source whose composition is similar to that of normal solar system material. An upper limit, at the 95% confidence level, is placed in the ratio of nuclei with $Z \geq 88/(74 \leq Z \leq 87)$ of 0.03.

1. Introduction

The heavy nuclei experiment on the HEAO-3 satellite was designed to determine the charge spectrum of cosmic ray nuclei from silicon to the actinides and to compare the elemental composition with those predicted for various hypothetical cosmic ray sources. In particular, the processes of nucleosynthesis that are responsible for the cosmic ray nuclei should determine the observed composition and hence be revealed by a measurement. Additionally, the heavy nuclei are strongly influenced by the processes of interstellar propagation and these processes can be investigated in terms of the various models of propagation.

This detector consisted of two pressure chambers, each containing two layers of x-y hodoscopes and three parallel plate ion chambers. Mounted between the chambers were two thin plastic Cherenkov radiators, Binns et al. (1981a). In orbit approximately 5×10^4 iron nuclei were detected per day. These nuclei have to satisfy the coincidence requirements that they transverse at least two of the four hodoscope layers and at least two of the seven charge measuring modules, but otherwise have no restrictions on angle or direction of motion. The minimum charge detectable is angle dependent but roughly corresponds to $Z \cong 14$, while a full scale signal would correspond to a nucleus of $Z \cong 120$ at 60°.

2. Experimental Data

As a consequence of the loose coincidence requirements imposed, the data obtained are of widely varying quality. The charge resolution

attainable depends critically on the subset of data chosen. For example, in the charge region $30 \leq Z \leq 40$, where the abundances are relatively large, it is possible to select a subset that contains only some 10% of the data and still obtain statistically significant abundances with individual charge resolution, Binns et al. (1981b). However, in the next charge region, $40 \leq Z \leq 58$, the same selection gives results of marginal statistical significance, while relaxing the selection criteria degrades the charge resolution. Fig. 1 shows the data for the high resolution selection and shows marginally significant abundance peaks at $_{50}$Sn and $_{56}$Ba.

The charge scale on Fig. 1 was derived assuming a strict Z^2 scaling from the normalization at the $_{26}$Fe peak. For these high Z nuclei, the energy loss equations would be expected to contain higher order Z terms due to the breakdown of the first Born approximation which in the limit requires that $Z/\beta << 137$. A summary of the theory has been given by Ahlen (1980), while Eby (1980) has calculated the effects that might be observed in our detectors. However, the validity of these corrections applied to a specific detector is not fully understood and ultimately a calibration, internal or external, will be essential. The effects of applying corrections based on the Ahlen formalism are shown in Fig. 1, where each particle has been re-assigned a charge based on its individual history. The result seems encouraging but unphysical. The small peaks at $_{50}$Sn and $_{56}$Ba appear better defined, but shifted in mean charge to non-integral and unreasonable charges. The magnitude of these corrections at these charges is quite small, but rapidly increases with increasing Z, becoming several charge units at $Z \cong 80$. Typical calculated values are shown in Fig. 2, for several energies and for charges determined from the Cherenkov signal, C, and from ion chamber signal combined with the Cherenkov signal, CI.

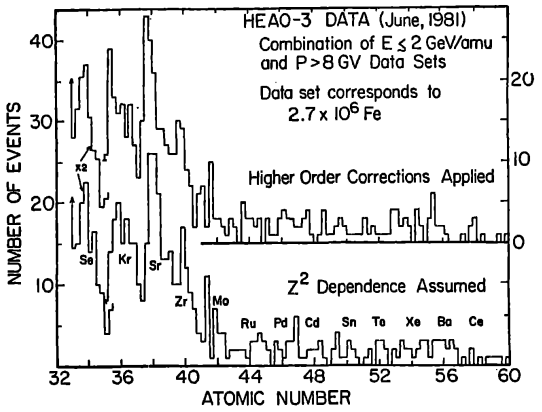

Fig.1. High resolution for $Z \lesssim 58$. Lower charge scale assumes only Z^2 scaling, upper includes higher order terms.

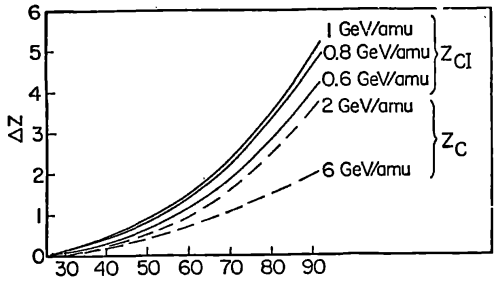

Fig.2. Charge overestimates due to assuming only Z^2 scaling as a function of Z.

3. Results

In order to obtain results of greater statistical significance, it is essential to relax the selection criteria and accept the resulting loss of charge resolution. The entire data set has been subdivided in some 25 bins, each characterized by various selection criteria. The

resolution and charge measurement obtained in each bin has been determined by examining the iron peak observed in that bin and the bins then ranked on the basis of the sharpness of the iron peak. In fig. 3 we show the charge spectra obtained for three groups of bins progressively

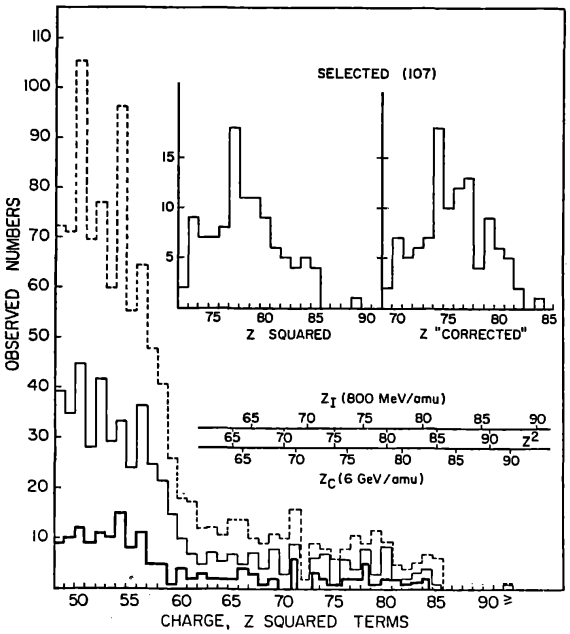

Fig.3. Charge spectra for three sets of data. Also shown are two alternative charge scales. The insets show the heaviest nuclei for two different charge assignments.

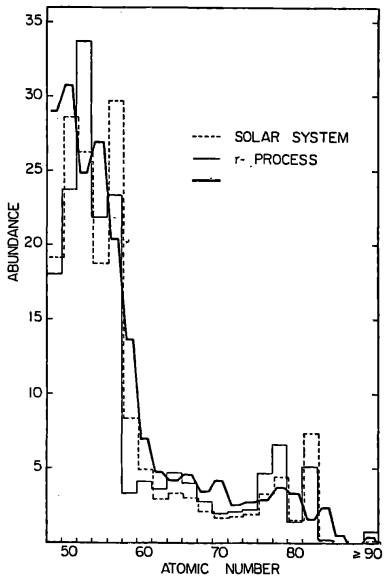

Fig.4. A comparison between predicted and measured charge spectra.

summing from the highest resolution set to those of lower resolution. No results are shown for bins characterized by an iron peak having $\sigma > 0.55$ charge units. These bins include 70% of the iron, or about 2×10^7 nuclei. This charge spectrum is based on charges assigned from a Z^2 scaling. Also shown are two alternative charge scales constructed from the curves in Fig. 2. It is clear that the net effect will be to smear any charge features in the $_{82}Pb$ - $_{78}Pt$ region. In order to examine this charge region with the best available statistics we have individually analyzed every event that was assigned a nominal charge of $Z \geq 72$ for what ever reason. The resulting charge spectrum of acceptable events is shown as the left hand insert to Fig. 3. The right hand insert shows the effect of correcting each charge assignment by the most appropriate of the two charge scales shown.

4. Discussion

The charge spectra shown in Fig. 3 can be compared with those expected from various assumed source spectra after propagation through the interstellar medium. Fig. 4 shows the spectra calculated by Brewster et al. (1981) after correction for the effects of the first ionization potential (4.30 exp (-0.18 I (eV))) and for propagation without energy loss through a simple leaky box with an escape path of 5 g/cm^2

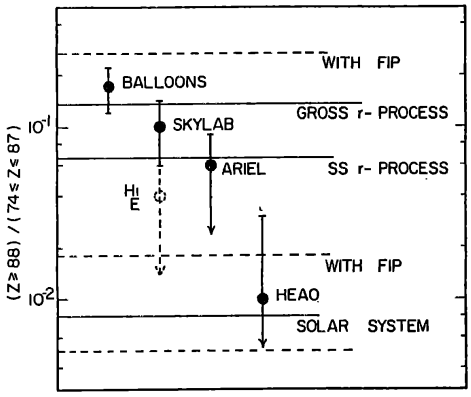

Fig.5. The actinide to lead-platinum ratio as observed and predicted.

of hydrogen. Spectra are shown assuming a solar system source composition, Cameron (1981), and an r-process source composition. For clarity, only the even-charged elements are shown, with the odd charge abundances divided equally, and the spectra are normalized to the abundances of the $50 \leq Z \leq 56$ elements.

The data shows the same main features as the predicted spectra, with a steep decline in abundance around $_{56}$Ba, an almost constant abundance in the lanthanides and subsidary Pt and Pb peaks, but is not in close correspondence with the details of either the r-process or SS prediction, nor could it be expected to until the charge assignments have been corrected. The insert of Fig. 3 shows that the ratio of $Z \geq 88/(74 \leq Z \leq 86)$, the "actinide to lead plus platinum" ratio is about 1%, with a 84% confidence upper limit of 3%. Fig. 5 shows a comparison of this result with some of those made by other workers and some of the predictions of Blake et al. (1978). These data show that while the earlier results were consistent with the predictions of a r-process source our own data has an upper limit that is clearly more consistent with a source having a solar system composition. This conclusion is not in disagreement with either the high energy Skylab data or the Ariel results.

5. Acknowledgments

This research was supported in part by NASA under contract NAS8-27976, 77, 78 and grants NGR 05-002-160, 24-005-050 and 26-008-001.

References

Ahlen, S.P., (1980), Rev. Mod. Phys. 52, 121.

Binns, W.R., et al., (1981a) Nucl. Instr. Meth. (to be published) (1981a) OG H.2-8.

Blake, et al., (1978), Ap. J. 221, 694.

Brewster et al., (1981), OG H.3-13.

Cameron, A.G.W., (1980), Center for Astroph. Reprint No. 1357.

Eby, P., (1980), private communication.

Fowler et al., (1981), Nature 291, 45. (Ariel)

Shirk, E.K. and P.B. Price, (1978), Ap. J. 220, 719. (Skylab)